Copy No. _____

Defence Research and Development Canada
Recherche et développement pour la défense Canada

DEFENCE R&D DÉFENSE

Modelling broadband scattering from shelled spheres in a waveguide

John A. Fawcett

Defence R&D Canada – Atlantic

Technical Memorandum
DRDC Atlantic TM 2007-270
October 2007

Canada

Modelling broadband scattering from shelled spheres in a waveguide

John A. Fawcett

Defence R&D Canada – Atlantic

Technical Memorandum

DRDC Atlantic TM 2007-270

October 2007

Author

Original signed by John A. Fawcett

John A. Fawcett

Approved by

Original signed by David Hopkin

David Hopkin
Head/Signatures

Approved for release by

Original signed by Jim L. Kennedy

Jim L. Kennedy
Head/Document Review Panel

Abstract

The broadband scattering characteristics of a target may be used to distinguish echos from a target of interest from those of clutter. This type of classification is of interest in many sonar applications: ASW, torpedo, surface mines, and diver detection. In a shallow water situation the original sonar pulse and the echo from the target will consist of a sequence of pulses corresponding to the various combinations of incident and backscattered multipath arrivals. For a very shallow target or one close to the seabed, it may be difficult to isolate some of these multipath arrivals. It is expected that these waveguide effects could have a significant effect upon some classifiers. In this paper, we discuss the modelling of scattering of sound from an elastic sphere (shelled, solid, water-filled, etc) which is in a waveguide with an upper surface and a lower seabed. An exact propagation solution is implemented and used to benchmark a ray-expansion solution. The scattered signals for a variety of different sonar pulses and different positions of a spherical target in the waveguide are shown.

Résumé

On peut se baser sur les caractéristiques de diffusion à large bande d'une cible pour faire la distinction entre les échos d'une cible d'intérêt et le clutter. Ce type de classification est utile dans bon nombre d'applications sonar : guerre anti-sous-marine, défense contre les torpilles, chasse aux mines de surface et détection des plongeurs. En eau peu profonde, l'impulsion sonar initiale et l'écho produit par la cible consistent en une séquence d'impulsions correspondant aux diverses combinaisons de signaux incidents et de signaux rétrodiffusés reçus par trajets multiples. Dans le cas d'une cible à très faible profondeur ou d'une cible à proximité du fond marin, il peut être difficile d'isoler certains de ces signaux reçus par trajets multiples. On prévoit que les effets de guide d'ondes pourraient avoir une incidence appréciable sur certains systèmes de classification. Le présent document traite de la modélisation de la diffusion du son par une sphère élastique (à coquille, pleine, remplie d'eau, etc.) comprise dans un guide d'ondes avec une surface supérieure et une surface inférieure constituée du fond marin. Une solution de propagation exacte est mise en œuvre et utilisée pour servir de référence à une solution de prolongement des rayons. Les signaux diffusés pour différentes impulsions sonar et différentes positions d'une cible sphérique dans le guide d'ondes sont présentés.

This page intentionally left blank.

Executive summary

Modelling broadband scattering from shelled spheres in a waveguide

John A. Fawcett; DRDC Atlantic TM 2007-270; Defence R&D Canada – Atlantic; October 2007.

Background

The detection and classification of a sonar echo is a problem of much interest for many sonar applications: ASW, torpedo defence, minehunting and diver detection. The ability to model a broadband signal scattered from a target in the oceanic waveguide is important in simulating data for sonar detection and classification studies. In this report, we consider a spherical scattering object located within a constant sound speed waveguide with an upper surface and lower seabed.

Principal results

It was found that it was possible to accurately and efficiently model the scattering from a spherical, shelled structure in a waveguide for a bandwidth of 80 Khz (or more). The effects of the waveguide on the resultant echo structure can be significant.

Significance of results

It is shown that in interpreting the sonar echos from objects in a waveguide, that the boundary interactions of the incident and scattered fields must be considered. The model of this report provides a way of accurately computing the broadband response of elastic, shelled spheres in a shallow water waveguide. The spectral content of the echo from a target can vary significantly with its depth and range in the waveguide or, in the time domain, the coherent combination of the echos from the various multipaths, can change the received pulse significantly from that which would be received in free space. This could lead to significant effects in terms of target detectability and could affect the classification of the object in the case that the classification was based upon the free space response of the target.

Future work

In future work, we would like to use the model of this report to generate data for detection and classification studies. Some simple experiments could establish the

validity of the model. The model could be extended to more general sound speed profiles by interfacing it with a ray-tracing code.

Sommaire

Modelling broadband scattering from shelled spheres in a waveguide

John A. Fawcett; DRDC Atlantic TM 2007-270; R & D pour la défense Canada – Atlantique; octobre 2007.

Introduction

La détection et la classification d'un écho sonar constituent un problème qui présente beaucoup d'intérêt dans bon nombre d'applications sonar : guerre anti-sous-marine, défense contre les torpilles, chasse aux mines et détection des plongeurs. La capacité de modéliser un signal à large bande diffusé par une cible dans le guide d'ondes océanique est importante pour la simulation des données destinées aux études de détection sonar et de classification. Dans le présent rapport, nous considérons un objet diffusant sphérique compris dans un guide d'ondes à vitesse du son constante avec une surface supérieure et une surface inférieure constituée du fond marin.

Résultats

On a constaté qu'il était possible de modéliser de manière précise et efficace la diffusion par une structure sphérique à coquille comprise dans un guide d'ondes pour une largeur de bande de 80 kHz (ou plus). Le guide d'ondes peut avoir une incidence appréciable sur la structure de l'écho résultant.

Portée

On montre que dans l'interprétation des échos sonar produits par des objets dans un guide d'ondes, les interactions aux limites des champs incidents et diffusés doivent être prises en compte. Le modèle du présent rapport permet de déterminer de manière précise la réponse à large bande de sphères à coquille élastiques dans un guide d'ondes en eau peu profonde. Le contenu spectral de l'écho produit par une cible peut varier de façon appréciable en fonction de sa profondeur et de sa distance dans le guide d'ondes ou, dans le domaine temporel, la combinaison cohérente des échos reçus par divers trajets multiples peut donner une impulsion grandement différente de l'impulsion qui aurait été reçue en espace libre. Cette situation peut avoir des effets marqués sur la détectabilité des cibles et influer sur la classification de l'objet lorsque la classification est basée sur la réponse en espace libre de la cible.

Recherches futures

Dans les recherches futures, nous aimerions utiliser le modèle du présent rapport pour générer des données destinées aux études de détection et de classification. Certaines expériences simples pourraient valider le modèle. Le modèle pourrait être étendu à des profils de vitesse du son plus généraux par son interfaçage avec un code de tracé de rayon.

Table of contents

List of figures

This page intentionally left blank.

1 INTRODUCTION

Over the last few years, there has been much interest in the discrimination of objects of interest from clutter on the basis of the spectral features of the received echo. This has been investigated for buried and proud mine and general target/clutter classification [1-4]. Unfortunately, a target's location within the ocean waveguide will also affect its echo characteristics. For example, in Ref. 5 it was shown how the echo from an aluminum sphere on a seabed, was significantly different in amplitude and phase, from that expected in free-space. Thus, an understanding of the target scattering process in a waveguide is important in understanding target detection and classification in a shallow water scenario.

In this report, the scattering solution for a sphere in a free space (i.e., just surrounded by a single homogeneous fluid) is described. The sphere can have an elastic shell and a different interior elastic fill. Thus, the model of the sphere is quite general and can model a possible target (for example, a steel shell surrounding an evacuated or filled interior) and clutter, a solid object, representing, perhaps, a rock. Some sample spectral and pulse computations are presented. This model is very efficient and can be used to model the spectral response of spherical targets up to, for example, hundreds of kilohertz [6].

The exact solution and approximations for target scattering in a waveguide have been discussed by a variety of authors [7-10]. Similar expression to the one in this report for the wavenumber approach can be found in [7-9]. However, this method begins to become computationally expensive for high frequencies or long ranges. In this report, we use a multipath ray expansion to describe the incident and scattered fields. A ray type approach was also used in Ref. 11 to model scattering from a rigid sphere in an oceanic waveguide and is used, in general, in many sonar performance models. In the present work, a systematic multipath expansion is used for the computation of the incident and scattered fields. The targets are taken to be general elastic-shelled spheres, possibly with an interior fill. The same general technique could be used with other target shapes, but the use of spheres allows for the scattering problem to be solved analytically and the symmetries of the spherical geometry make some of the computations easier.

In the numerical examples, some example spectral and pulse computations are considered for a steel-shelled sphere in free space. Then the sphere is considered in a shallow waveguide with a bottom, penetrable seabed and a top pressure release surface. A point source is considered at a specified depth. The resulting scattered pressure fields as computed by both the wavenumber integral and the multipath ray approaches are shown as a function of the sphere depth. In the case of the wavenumber integral approach, the effect of including rescattering terms is also investigated. The ray method is then used to compute the received echo time series for various ranges and depths

of the sphere.

2 Theory

2.1 Scattering from a sphere in free space

The pressure field incident upon a sphere in free space, due to a point source at (R_S, ϕ_S, θ_S), can be expressed in terms of spherical Hankel/Bessel and Legendre Functions as

$$\begin{aligned} P^{inc}(R,\phi,\theta) &= ik\sum_{m=0}^{\infty}\sum_{n=m}^{\infty}\epsilon_m h_n(kR_S)j_n(kR) \\ &\times \; P_n^m(\cos\phi_S)P_n^m(\cos\phi)\cos m(\theta-\theta_S) \end{aligned} \tag{1}$$

where $k = 2\pi f/c$ and $\epsilon_m = 2$ for $m > 0$ and ϵ_m =1 for $m = 0$. In this report we use the normalization that

$$P_n^m(x) = \sqrt{2n+1}\sqrt{\frac{(n-m)!}{(n+m)!}}\tilde{P}_n^m(x) \tag{2}$$

where $\tilde{P}_n^m(x)$ are the standard Legendre Functions. The expansion of Eq.(1)is based upon the origin of the coordinate system being at the centre of the sphere. The variable R is the three-dimensional range. The variable ϕ is the polar angle measured off the vertical angle and θ is the azimuthal angle around the vertical axis. The subscript S denotes the coordinates of the source as measured from the origin. In the case that ϕ_S is taken to be zero (i.e., the source is taken to lie upon the axis passing through the sphere) then this expression simplifies to

$$p^{inc}(R,\phi) = ik\sum_{n=0}^{\infty}\sqrt{(2n+1)}h_n(kR_S)j_n(kR)P_n(\cos\phi). \tag{3}$$

The field scattered by a sphere is then given by, in the case of Eq.(1)

$$p^{sc}(R,\phi,\theta) = \sum_{m=0}^{\infty}\sum_{n=m}^{\infty}a_n p_{nm}^{inc}P_n^m(\cos\phi)h_n(kR) \tag{4}$$

or, for Eq.(3),

$$p^{sc}(R,\phi) = \sum_{n=0}^{\infty}a_n p_n^{inc}h_n(kR)P_n(\cos\phi). \tag{5}$$

In these equations the terms p_{nm}^{inc} and p_n^{inc} denote the incident coefficients of $j_n(kR)p_n^m(\cos\phi)$ as defined by the expressions of Eqs.(1) and (3). The scattering process of the sphere is characterized by the scattering coefficients a_n. For example, in the case of a rigid sphere,

$$a_n = \frac{-j_n'(kR_0)}{h_n'(kR_0)}. \tag{6}$$

In the case of an elastic shelled sphere with possibly an internal elastic fill, a vector of coefficients are obtained by solving a 7×7 system of equations for each order n. There are the unknown coefficients of the spherical Hankel functions in the surrounding fluid. The compressional and shear potentials in the shell each have coefficients for spherical Hankel and Bessel functions. In the interior, there are unknown coefficients for the spherical Bessel functions for the compressional and shear potentials. There are no spherical Hankel functions here as they are singular at the origin. The continuity of displacements and stresses at the interfaces yield the necessary equations to determine all the coefficients at each order n. In particular, we are interested in the coefficients of the spherical Hankel functions in the fluid surrounding the sphere. Once these coefficients have been obtained then the scattered field can be computed anywhere in the surrounding free space.

However, when the sphere is in a waveguide, the situation is more complicated. The field incident upon the sphere includes the propagation effects of the energy in the waveguide. The field scattered by the sphere also interacts with the waveguide before arriving at the receiver. In addition, some of the scattered energy will reflect off the boundaries and be reincident upon the sphere and this will lead to a sequence of interactions between the sphere and the boundaries.

2.2 Scattering from a sphere in a waveguide - an exact wavenumber integral expression

In this section, we derive an expression for the scattering from a sphere in a waveguide. This problem has been addressed in various forms by previous authors [5,7-10]. The derivation below leads to the various wavenumber integrals which we implemented numerically. In order to derive the scattering from a sphere in a waveguide, we consider as a starting point, Eq.(1), for the pressure field scattered by the sphere. We take the polar angle, ϕ, to be measured off the vertical axis z. The term $h_n(kR)P_n^m(\cos\phi)$ can be written for $z < 0$ as

$$h_n(kR)P_n^m(\cos\phi) = i^{n-m}\int_0^\infty \frac{qJ_m(qr)e^{-i\gamma z}}{k\gamma}P_n^m(\frac{\gamma}{k})dq \tag{7}$$

and for $z > 0$,

$$h_n(kR)P_n^m(\cos\phi) = i^{n-m}\int_0^\infty \frac{qJ_m(qr)e^{i\gamma z}}{k\gamma}P_n^m(\frac{-\gamma}{k})dq \tag{8}$$

where $k \equiv 2\pi f/c$ and $\gamma = \sqrt{k^2 - q^2}$. These two expressions represent downgoing and upgoing wavefields respectively. Because of the interactions with the top and bottom boundaries of the waveguide, these fields, for each value of the wavenumber parameter q will be modified by a series of reflections off the top and bottom of the

waveguide. There will be 4 wavenumber integrals expressing the propagation of the (nm) Spherical Harmonic,

$$T_1 = i^{n-m} \int_0^\infty \frac{qJ_m(qr)}{k\gamma} \frac{R(q)}{1 + R(q)e^{i2\gamma h}} P_n^m(\gamma/k) \exp(i\gamma(2D + z_{rec}))dq, \tag{9}$$

$$T_2 = i^{n-m} \int_0^\infty \frac{qJ_m(qr)}{k\gamma} \frac{-R(q)}{1 + R(q)e^{i2\gamma h}} P_n^m(\gamma/k) \exp(i\gamma(2h - z_{rec}))dq, \tag{10}$$

$$T_3 = i^{n-m} \int_0^\infty \frac{qJ_m(qr)}{k\gamma} \frac{-1}{1 + R(q)e^{i2\gamma h}} P_n^m(-\gamma/k) \exp(i\gamma(2h - 2D - z_{rec}))dq, \tag{11}$$

and

$$T_4 = i^{n-m} \int_0^\infty \frac{qJ_m(qr)}{k\gamma} \frac{-R(q)}{1 + R(q)e^{i2\gamma h}} P_n^m(-\gamma/k) \exp(i(2\gamma h + z_{rec}))dq. \tag{12}$$

Here h is the depth of the waveguide, D is the distance of the sphere from the seabed, and z_{rec} is the vertical coordinate of the receiver, relative to the sphere centre. The term $R(q)$ is the reflection coefficient for the bottom seabed and for a simple homogeneous seabed has the form,

$$R(h) = \frac{(\rho_2\gamma_1 - \rho_1\gamma_2)}{(\rho_2\gamma_1 + \rho_1\gamma_2)}. \tag{13}$$

with $\gamma_1 \equiv \sqrt{\omega^2/c_1^2 - q^2}$ and $\gamma_1 \equiv \sqrt{\omega^2/c_2^2 - q^2}$. In the propagation of the scattered field, each of the above terms is multiplied by $a_n p^{inc}(nm)$, the incident field coefficient for the (nm) Spherical Harmonic multiplied by the sphere scattering coefficient a_n. For the mth azimuthal order, these propagation terms are summed with respect to the index n. Thus, for example, the summation of T_1 results in the propagation integral

$$\tilde{T}_1 = \int_0^\infty \frac{qi^{m+1}F_m(q)J_m(qr)}{k} \frac{R(q)}{1 + R(q)e^{i2\gamma h}} P_n^m(\gamma/k) \exp(i\gamma(2D + z_{rec}))dq, \tag{14}$$

where

$$F_m(q) = \sum_{n=m}^{\infty} a_n \frac{P_n^m(\mp\gamma/k)}{\gamma} \cos(m\pi) p^{inc}(nm) \tag{15}$$

In Eq.(15) the negative sign is used with the Legendre Function, if the sign is positive in Eqs.(9)-(12) and vise versa. We chose to write the expression for F_m in this manner as it is the Scattering Function for the sphere, for the mth azimuthal order, in the polar direction $\phi = \gamma/k, \theta = \pi$.

The first of the 4 expressions, Eq.(9) represents a reflection off the seabed of the scattered field and then 1,2,... reflections off the water/air and seabed interfaces before arriving at the receiver. The second integral, Eq.(10), is the same except that there is an additional reflection off the top pressure release surface before the scattered energy arrives at the receiver. The third and fourth terms represent energy initially scattered upwards from the sphere with a sequence of reflections off the top and bottom surfaces before arriving at the receiver with an additional final reflection off the bottom seabed in the fourth expression. There is also the direct term, representing the free space scattering term which does not undergo any interaction with the boundaries before reaching the receiver and for this we could use a wavenumber integral. However, we simply use an expression of the form of Eq.(5) for this term. The final expression for the backscattered field is then given by

$$p^{sc}(r, z_{rec}) = \tilde{T}_1 + \tilde{T}_2 + \tilde{T}_3 + \tilde{T}_4 + T_D \tag{16}$$

where T_D is the direct propagation of the scattered field to the receiver. This direct term can be expressed as the sum of the scattered spherical harmonics, (Eq.(4)).

It is interesting to reexpand the integrals of Eqs.(9) - (12) in terms of incoming spherical harmonics $j_n(kR)P_n^m(\cos\phi)$. In order to do this, the relation

$$J_m(hr)e^{i\gamma z} = \sum_{n=m}^{\infty} i^{(n-m)} P_n^m(\cos\phi) P_n^m(\gamma/k) j_n(kR), \tag{17}$$

is used. Then these integrals can be written as

$$T_1 = \sum_{v=m}^{\infty} i^{v+n-2m} j_v(kR) P_n^m(\cos\phi) \int_0^{\infty} \frac{qe^{2i\gamma D}}{k\gamma} \frac{R(q)}{1+R(q)e^{2i\gamma h}} P_v^m(\gamma/k) P_n^m(\gamma/k) dq \tag{18}$$

$$T_2 = \sum_{v=m}^{\infty} i^{v+n-2m} j_v(kR) P_n^m(\cos\phi) \int_0^{\infty} \frac{qe^{2i\gamma h}}{k\gamma} \frac{-R(q)}{1+R(q)e^{2i\gamma h}} P_v^m(-\gamma/k) P_n^m(\gamma/k) dq \tag{19}$$

$$T_3 = \sum_{v=m}^{\infty} i^{v+n-2m} j_v(kR) P_n^m(\cos\phi) \int_0^{\infty} \frac{qe^{2i\gamma(h-D)}}{k\gamma} \frac{-1)}{1+R(q)e^{i2\gamma h}} P_v^m(-\gamma/k) P_n^m(-\gamma/k) dq \tag{20}$$

$$T_4 = \sum_{v=m}^{\infty} i^{v+n-2m} j_v(kR) P_n^m(\cos\phi) \int_0^{\infty} \frac{qe^{2i\gamma h}}{k\gamma} \frac{-R(q))}{1+R(q)e^{i2\gamma h}} P_v^m(\gamma/k) P_n^m(-\gamma/k) dq \tag{21}$$

From these sums, it can be seen that an outgoing Spherical Harmonic function $h_n(kR)P_n^m(\cos\phi)$ is converted into a set of incoming Spherical Harmonics from the reflections off the surrounding boundaries. After truncating the set of outgoing and

incoming harmonics, this conversion process, at order m can be expressed by a conversion matrix,

$$v^{in}(n) = \mathbf{C_m} v^{out}(n), \quad n = m, ..., N \tag{22}$$

where v^{in} is the vector of incoming coefficients, v_{out} is the vector of scattering coefficients for $h_n(kR)P_n^m(\cos\phi)$ and v^{inc} will represent the original incident coefficients. The $(v, n), (v, n \geq m)$ element of the conversion matrix C_m is computed by taking the (v-m+1)th term of $T_1 + T_2 + T_3 + T_4$ in Eqs.(18)-(21) which represent the conversion of the outgoing Spherical Harmonic, $h_n(kR)P_n^m(\cos\phi)$.

In free space, the scattering process for the harmonics of the mth azimuthal order can be expressed with a diagonal scattering matrix D whose entries are the scattering coefficients $a_n, n = m, ..., N$. However, because of the additional conversion process described above, the effective scattering from the sphere is given by a sum of a series of scattering and rescattering,

$$v^{out} = (D + DC_mD + DC_mDC_mD + ...)v^{inc} \tag{23}$$

or

$$v^{out} = (D^{-1} - C_m)^{-1} v^{inc} \tag{24}$$

If one ignores the conversion matrix C_m (the single scatter approximation) then Eq.(24) reduces to $v^{out} = Dv^{inc}$. In the computation of the scattering function $F_m(q)$ of Eq.(15) one can ignore the rescattering of energy onto the sphere by the surrounding boundaries and simply use the coefficients $a_n, n = m, ..., \infty$ or one can compute the effective new coefficients using Eq.(24).

In the case that the incident field is a plane wave then $v^{inc}(n)$ can be specified analytically. However, in this report, the incident field is taken to come from a point source in the waveguide. In this case, the mth azimuthal component of the incident field can be written as

$$\begin{aligned} p^{inc}(r, z; m) &= ik \sum_{n=m}^{\infty} P_n^m(\cos\phi_s) P_n^m(\cos\phi) h_n(kR_s) j_n(kR) + i \int_0^{\infty} \frac{J_m(qr_s) J_m(qr)}{\gamma} \\ &\times \frac{\hat{T}_1(q)e^{i\gamma z} + \hat{T}_2(q)e^{-i\gamma z} + \hat{T}_3(q)e^{-i\gamma z} + \hat{T}_4(q)e^{i\gamma z}}{1 + R(q)e^{i2\gamma h}} qdq \end{aligned} \tag{25}$$

where R_s and ϕ_s are the source coordinates meaured from the centre of the sphere and the terms $\hat{T}_1, \hat{T}_2, \hat{T}_3, \hat{T}_4$ are given by

$$\hat{T}_1(q) = R(q)\exp(i\gamma(D + z_{rec})) \tag{26}$$

$$\hat{T}_2(h) = -R(q)\exp(i\gamma(D + 2h - z_{rec})) \tag{27}$$

$$\hat{T}_3(q) = -\exp(i\gamma(2h - D - z_{rec})) \tag{28}$$

$$\hat{T}_4(q) = \exp(i\gamma(z_{rec} + 2h - D)) \tag{29}$$

Using the relation from Eq.(17), we can write that the incident term for $P_n^m(\cos\phi)j_n(kR)$ is given by

$$\begin{aligned} p_{nm}^{inc} &= i^{n-m}\int_0^\infty \frac{(\hat{T}_1(q)+\hat{T}_4(q))P_n^m(\gamma/k)+(\hat{T}_2(q)+\hat{T}_3(q))P_n^m(-\gamma/k)}{\gamma(1+R(q)e^{2i\gamma h})}J_m(qr_s)qdq \\ &+ ikP_n^m(\cos\phi_s)h_n(kR_S) \end{aligned} \tag{30}$$

This expression when combined with those of Eqs.(15) and Eqs.(9) - (12) could be expressed as double integrals and expressions similar to those of this report can be found expressed in Ref.9. However, in this report the scattered field is computed in the manner outlined above. First, the incident coefficients are computed using the expression(s) given by Eq.(30). These coefficients, can then be modified by Eq.(24), if the rescattering effects are desired. The resulting scattering coefficients are used in the computation of $F_m(h)$ in Eq.(15) and the evaluation of the scattering integrals of the form of Eq.(14). Once the scattered fields $P_m^{sc}(r,z)$ have been computed for all azimuthal orders m, the final result is computed from

$$P(r,z,\theta)=\sum_{m=0}^{\infty}\epsilon_m P_m^{sc}(r,z)\cos m\theta \tag{31}$$

where in our examples $\theta = 0$.

2.3 Scattering from a sphere in a waveguide - a multipath expression

The multipath expansion expression for propagation in a Pekeris waveguide is well known [12] and we can write

$$p(r,z)=\frac{e^{ikD_D}}{D_D}+\sum_{n=0}^{\infty}V_1(n)\frac{e^{ikD_{n1}}}{D_{n1}}+V_2(n)\frac{e^{ikD_{n2}}}{D_{n2}}+V_3(n)\frac{e^{ikD_{n3}}}{D_{n3}}+V_4(n)\frac{e^{ikD_{n4}}}{D_{n4}} \tag{32}$$

where

$$D_{n1} = \sqrt{r^2+(z+z_s+2(n-1)h)^2} \tag{33}$$

$$D_{n2} = \sqrt{r^2+(z-z_s-2nh)^2} \tag{34}$$

$$D_{n3} = \sqrt{r^2+(-z-z_s+2nh)^2} \tag{35}$$

$$D_{n4} = \sqrt{r^2+(z-z_s+2nh)^2} \tag{36}$$

and D_D is the distance of the direct arrival. The coefficients are given by

$$V_1(n) = R^n(\theta_{1n})(-1)^{n-1} \tag{37}$$

$$V_2(n) = (-R(\theta_{2n}))^n \tag{38}$$

$$V_3(n) = (-1)^n R(\theta_{3n})^{n-1} \tag{39}$$

$$V_4(n) = (-R(\theta_{4n}))^n \tag{40}$$

Here the angles θ_{1n}, θ_{2n}, etc. denote the angle that the ray makes with bottom seabed and they are given by

$$\theta_{jn} = Acos(\frac{r}{D_{jn}}). \tag{41}$$

and R denotes the seabed reflection coefficient for this angle. We will consider N rays of each of the 4 ray families in addition to the direct ray, resulting in $4N + 1$ rays and these will simply be denoted with an index $k = 1, ..., 4N + 1$ with $k = 1$ being the direct term.

Using this approach, the rays incident upon the sphere from the specified source position are computed. Then the same geometric set of rays are considered the propagate the scattered field from the sphere back to the source. This approach is correct for the monostatic case. For the bistatic case, this second set of rays would correspond to those joining the sphere centre to the specified receiver position(s). Thus we can write for the scattered field,

$$p^{sc}(r, z) = \sum_{n_1=0}^{4N+1} \sum_{n_2=0}^{4N+1} V(n_1)V(n_2)\frac{\exp(ik(D_{n1} + D_{n2}))}{D_{n1}D_{n2}} S(\phi_{n2} - \phi_{n1}). \tag{42}$$

In Eq.(42) $S(\phi)$ denotes the farfield free space scattering pattern for the sphere and due to the symmetries of the sphere, this function depends upon only the one angle, the difference between the incoming and outgoing angles. It is important that these angles are defined in such a way that the difference is correct. For example, for the ray scattered upwards from the sphere and then reflecting off the top pressure release surface for the $n3$ family of Eq.(35), the angle is given by

$$\phi = Acos((2nh - z - z_s)/D_{n3}) \tag{43}$$

whereas for a seabed reflected ray of Eq.(33), the angle is given by

$$\phi = \pi - Acos((z + z_s + 2(n - 1)h)/D_{n1}). \tag{44}$$

The far field scattering pattern $S(\phi)$ is given by

$$S(\phi) = -i\sum_{n=0}^{\infty} a_n \frac{\sqrt{(2n + 1)}}{k}(-1)^n P_n(\cos\phi)) \tag{45}$$

Although the multipath approach is pleasing intuitively, it is not clear that it is mathematically correct. However, as is done in [12], in the wavenumber integrals in the previous expansion, the term $1/(1 + R(q)e^{i2\gamma h})$ can be expanded as

$$1/(1 + R(q)e^{i2\gamma h}) = 1 - R(q)e^{i2\gamma h} + R^2(q)e^{i4\gamma h} + ... \tag{46}$$

Each of these new integrals can be treated, using the method of Stationary Phase and the asymptotic behaviour of J_m, to obtain, in the end, the ray expansion just described (note, for example, in Eq.(15) that we wrote the factor $F_m(q)$ in terms of the scattering pattern for the sphere). Alternatively, one could use the same approach as Ingenito [13]. Although he used a modal representation, he interpreted the scattering in terms of the modes having equivalent ray directions and being a combination of plane waves.

In the monostatic case, Eq.(42) can be rewritten as

$$p^{sc}(r,z) = \sum_{n_1=0}^{4N+1} \sum_{n_2=n_1}^{4N+1} w(n_1,n_2) V(n_1) V(n_2) \frac{\exp(ik(D_{n1}+D_{n2}))}{D_{n1} D_{n2}} S(\phi_{n2} - \phi_{n1}), \quad (47)$$

where $w(n_1, n_2) = 1$ for $n_1 = n_2$ and $w(n_1, n_2) = 2$ otherwise. Although, we will not consider a moving source in this report, the form of Eq.(47) is very amenable to considering a doppler shift for each combination of ray path.

3 NUMERICAL EXAMPLES

We start by considering scattering from an elastic-shelled and a rigid sphere in free space. The sphere is 0.25 m in radius. The shell is 6 mm thick and is steel. The interior of the sphere is taken to be a vacuum. The scattering coefficients a_n are computed for 8001 frequencies at an increment of 10 Hz for both the shelled and rigid case. The rigid ease eorresponds to the normal derivative of the pressure vanishing at the surface of the sphere. In this case, the scattering coeffieients are given analytically by

$$a_n = -\frac{j_n'(kR_0)}{h_n'(kR_0)}. \tag{48}$$

The eoefficients in the ease of an elastie-shelled sphere are eomputed using an existing FORTRAN eode. For the ease of the sphere in a waveguide, these coefficients are read in as a file for the MATLAB code which then uses them in the waveguide eomputations using either the wavenumber integral approach or the multipath-ray approach. In Fig. 1 the spectrum of the backscattered field at a range of 100 m is shown for the shelled sphere in blue and for the rigid sphere in red. There are strong resonance features for the shelled sphere. In Fig. 2 we show the computed backscattered timeseries for an incident pulse of the form

$$S(f) = \exp(-(f - f_c)^2/(2(BW/2)^2)), \quad f > 0 \tag{49}$$

where $f_c = (f_1 + f_{end})/2$ and $BW = (f_{end} - f_1)$. For all the pulses $f_1 = 100Hz$ with f_{end} = 4100 Hz, 8100Hz, and 16100 Hz. The left hand column shows the time series for the elastic shelled sphere and the right hand column shows the response for the rigid sphere. It is elear that there is significant return for the shelled sphere for several milliseconds after the specular return, particularly for the lowest frequency pulse centred at about 2 kHz. In Fig. 3, a zoom of the region near the specular reflection is shown for the elastic and rigid spheres for the [100 16100] Hz pulse. The specular reflection for the shelled sphere has the opposite polarity than that of the rigid sphere. This is because the shell is still relatively thin at this frequeney and the interior of the sphere is a vacuum. The rigid sphere has a small secondary arrival after the speeular reflection - this is the Franz wave arrival [14].

The seattering coefficients $a_n(\omega)$ for the elastic shelled sphere are now used in conjunction with Eqs.(15) and (16) to compute the scattered field using the wavenumber integral approach and also with the ray-based approach. The seabed has a sound speed of 1700 m/s and a density of ρ = 1.5 g/cm^3. The depth of the oeean waveguide is 30 m. The source is located at a depth of 15 m. The sphere is located at a horizontal range of 100 m and its depth is varied between 0.3 to 29.7 m. The scattered field is computed for 2001 frequencies in the range [100 4100] Hz. In Figs. 4 and 5, we show a comparison of the computed backscattered spectra (multiplied by 10^4

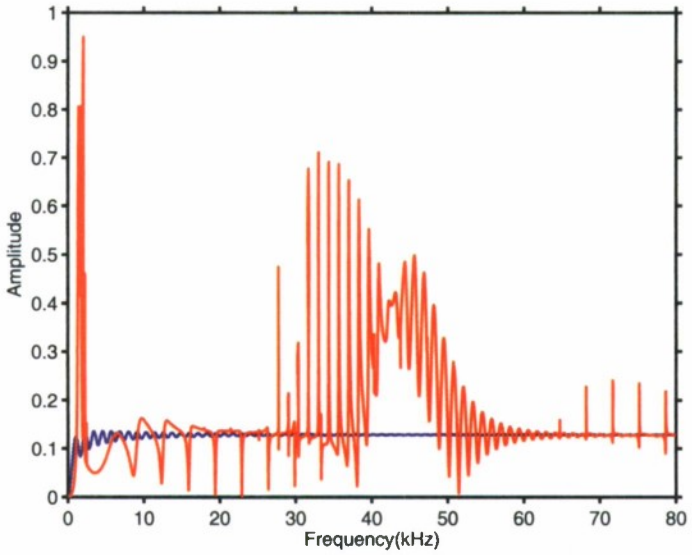

Figure 1: *The backscattered spectrum (free space) for an elastic-shelled sphere (red), 0.25 m in radius and a rigid sphere (blue)*

to compensate for range) for sphere centres depths ranging from 0.25 m to 29.75 m. The depth of 0.25 m means that the sphere is just touching the upper pressure release surface and the depth of 29.75 m signifies the sphere touching the seabed. In Figs. 6 and 7, the resulting time series, using the source function of Eq.(49) with a bandwidth of 4 kHz, are shown. As can be seen, the inclusion of the rescattering effects has a significant effect for the sphere close to the upper surface. This effect dies away rapidly as the sphere centre goes more than about 40 cm from the surface. For this particular example, the rescattering terms do not have a significant effect for the sphere close to the seabed. However, it is not clear that this will always be the case. In fact, since the bottom seabed can be made to approximate either a pressure release or rigid surface, this will definitely not always be the case.

In the following computations, we will ignore the rescattering terms. However, it should be noted that for the sphere within small distances of the free surface (and perhaps, the seabed) these results may not be accurate. It is possible to include these effects in the ray-based model by including these terms and computing a two-dimensional scattering function $S(\phi_{out}, \phi_{in})$ (the scattering function would no longer simply depend upon the difference of angles) . In the case of varying target position this would be time-consuming, as the rescattering coefficients would need to be re-computed for each new target position. In the case when the target position is fixed and the receiver or source position varied, this might be a feasible approach.

In Fig. 8 we show a comparison between the results obtained from the wavenumber method (no rescattering) and the multipath expansion method. Here, at 100 Hz,

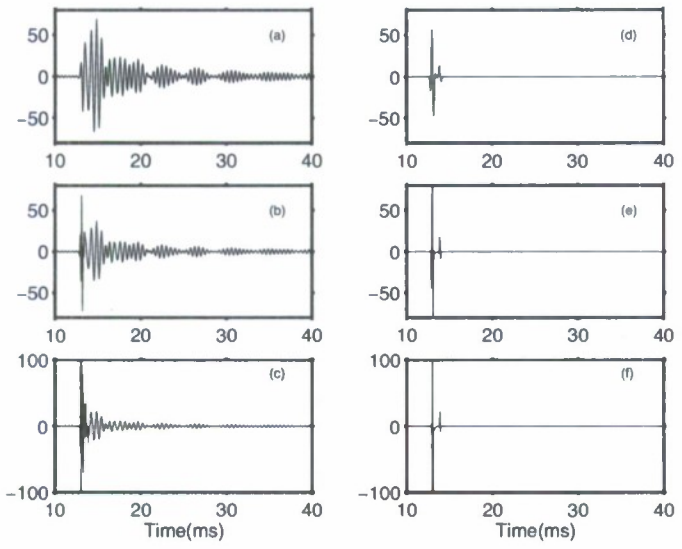

Figure 2: *The computed backscattered time series for a Gaussian weighted spectrum - elastic response shown in (a)-(c) for frequencies in [100 4100]Hz, [100 8100] Hz and [100 16100] Hz. The corresponding rigid results are shown in (d)-(f)*

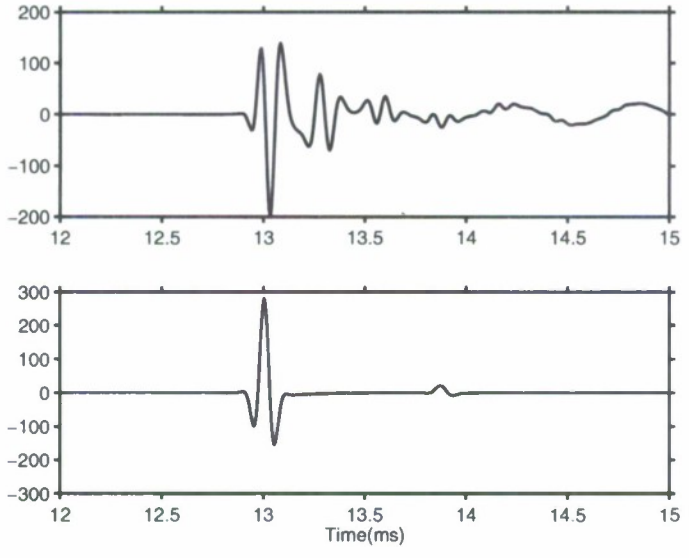

Figure 3: *A detailed look at the region of the specular reflection for Figures (c) and (f) of Fig.3 for the elastic shelled and rigid spheres. The frequency range is [100 16100] Hz.*

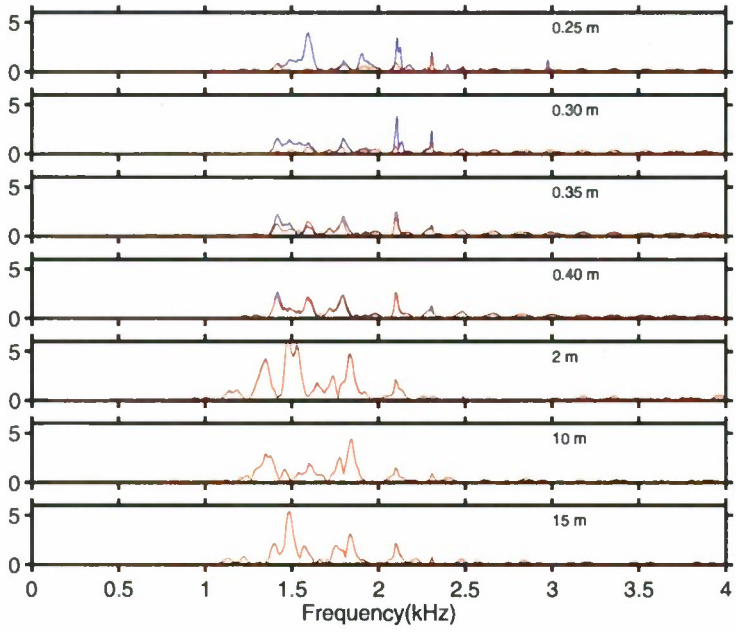

Figure 4: *A comparison of the spectra as a function of sphere depth with rescattering terms (blue) and without rescattering (red)*

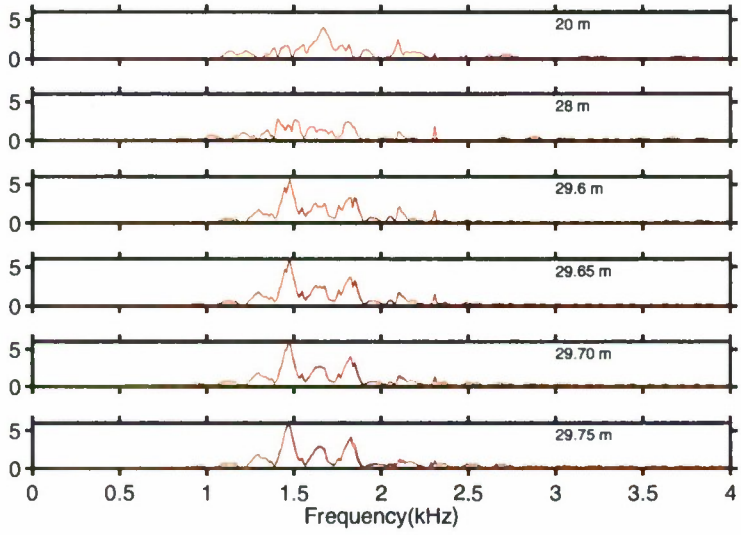

Figure 5: *A comparison of the spectra as a function of sphere depth with rescattering terms (blue) and without rescattering (red)*

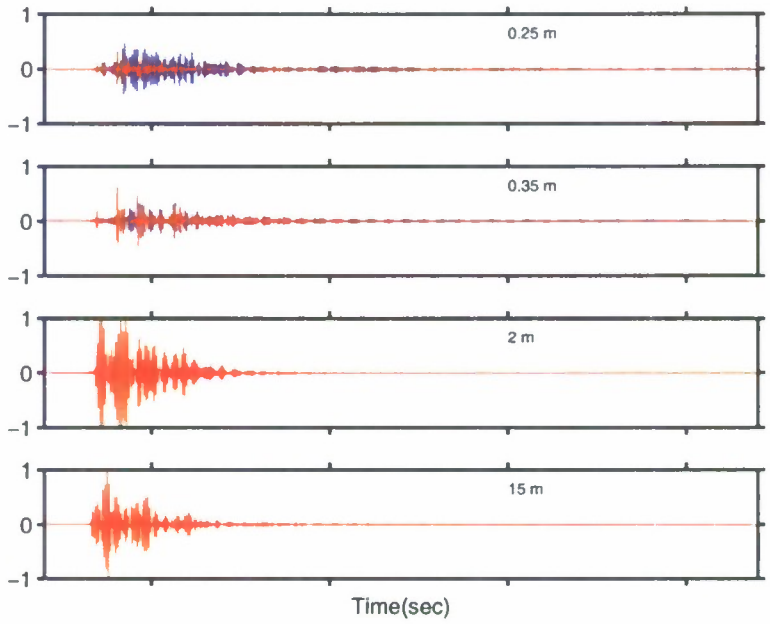

Figure 6: *A comparison of the time series as a function of sphere depth with rescattering terms (blue) and without rescattering (red)*

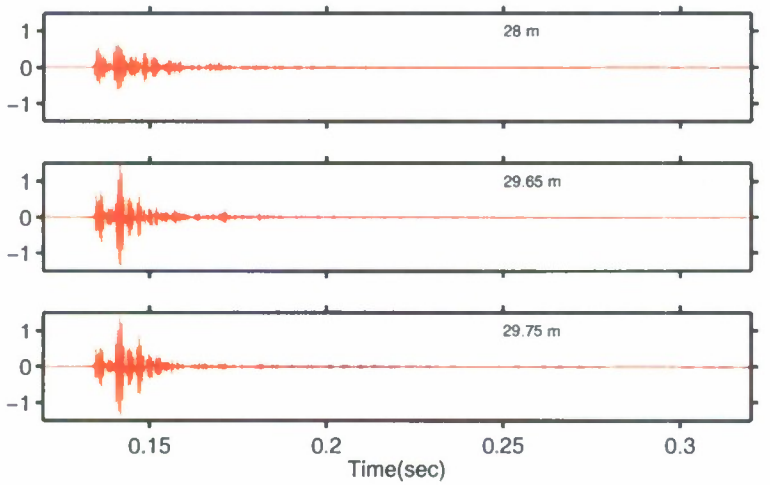

Figure 7: *A comparison of the time series as a function of sphere depth with rescattering terms (blue) and without rescattering (red)*

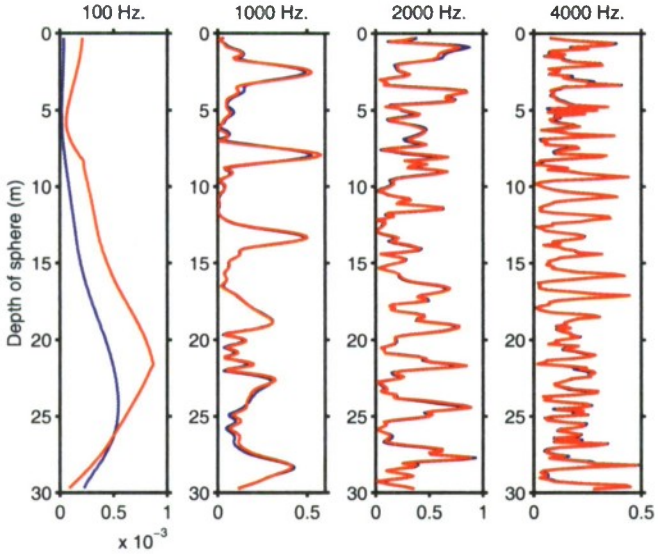

Figure 8: *The scattered field amplitude (multiplied by 10^4) as computed by wavenumber integral approach (blue) and the multipath approach (red) as a function of sphere depth. The source/receiver depth is 15 m and the range to the sphere is 100 m.*

there is a significant disagreement between the results. This is not surprising. The multipath expansion approach is a high frequency approach. For example, the behaviour of the wavenumber integral near the critical point is not accounted for and effects such as beam displacement[15] are ignored. The multipath curve shows 2 slight "kinks" near 8.3 and 21.7 m. These correspond to depths for which there are 2 bottom reflections with an angle very close to the critical angle for this seabed. However, by 1000 Hz, the 2 results are nearly identical. In Fig. 9 we show a comparison of the 2 curves for 100 - 400 Hz. In this case, there is still disagreement between the curves at 200-400 Hz, but they are much closer than at 100 Hz.

In Fig. 10 we show a two-dimensional plot of the received spectra, computed using the multipath expansion method as a function of frequency and sphere depth and in Fig. 11 we show the resulting time series computed using Fourier synthesis. In both plots one can see the significant effect of the sphere depth on the character of the received signal and also the semi-periodic appearance. In Fig. 12 we show in (a) the direct echo pulse, in (b) the time series for a sphere at 0.3 m depth (c) for the sphere at 15 m depth and (d) the sphere at 29.7 m depth (i.e., just above the seabed). Once again, the large variation of the echo with sphere depth is seen as well as the significant change from the echo which would be received in free space.

We now show the spectral plot and time series for the case of the sphere at 600 m range. It is interesting to consider how many multipath terms are required to obtain an accurate pressure computation. Let us suppose that θ_c denotes the critical angle

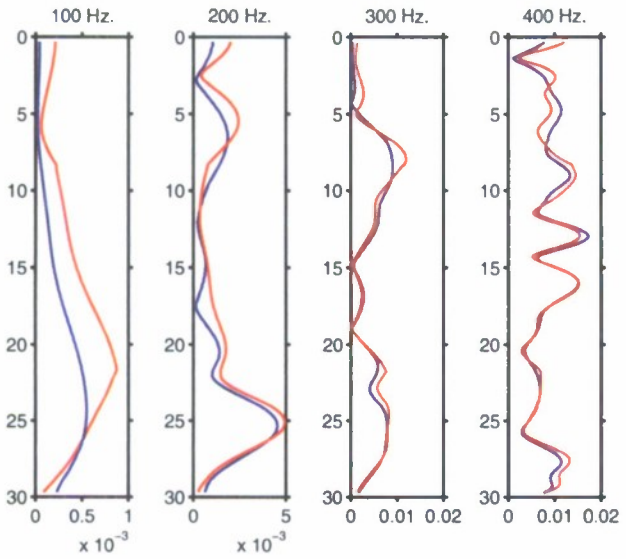

Figure 9: *The scattered field amplitude (multiplied by 10^4) as computed by wavenumber integral approach (blue) and the multipath approach (red) as a function of sphere depth. The source/receiver depth is 15 m and the range to the sphere is 100 m.*

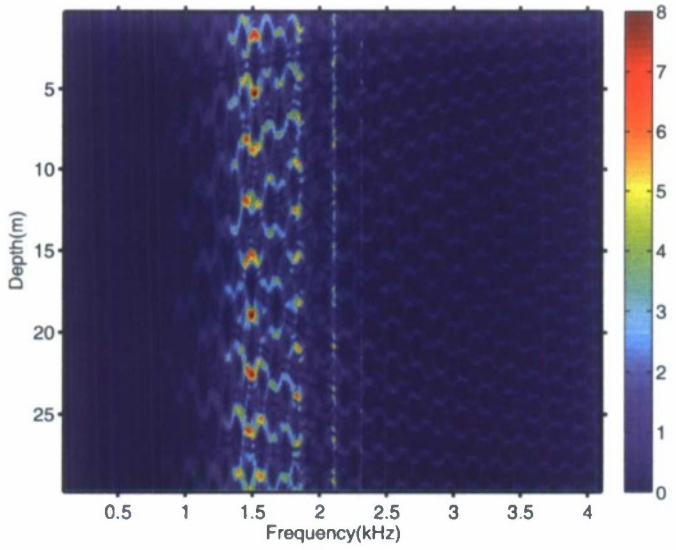

Figure 10: *The scattered field amplitude (scaled by 10^4) as function of frequency and sphere depth*

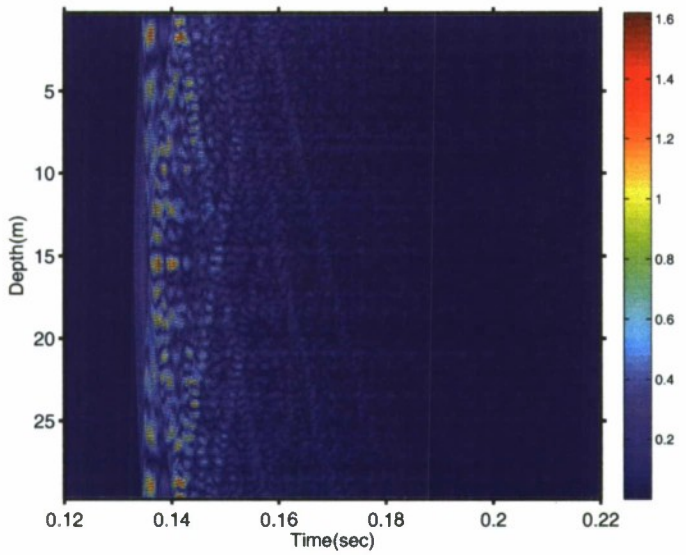

Figure 11: *The scattered field time series (amplitude) as a function of sphere depth.*

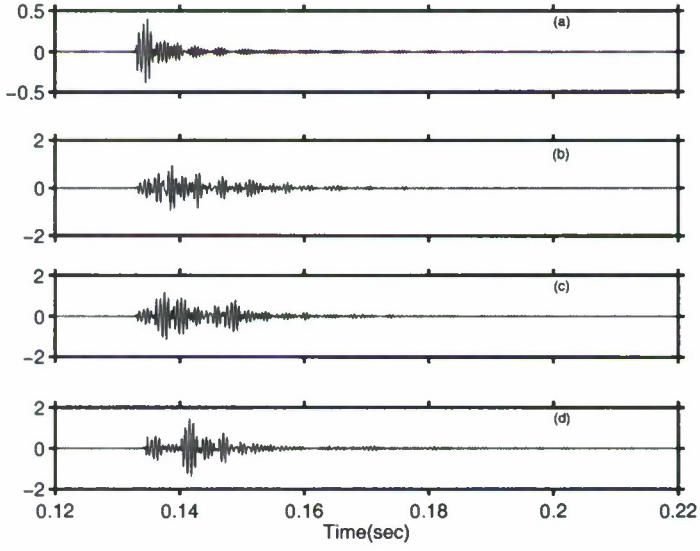

Figure 12: *Representative time series for (a) the free space echo (b) the sphere at 10 depth (c) the sphere at 15 m depth and (d) the sphere at 29.7 m depth*

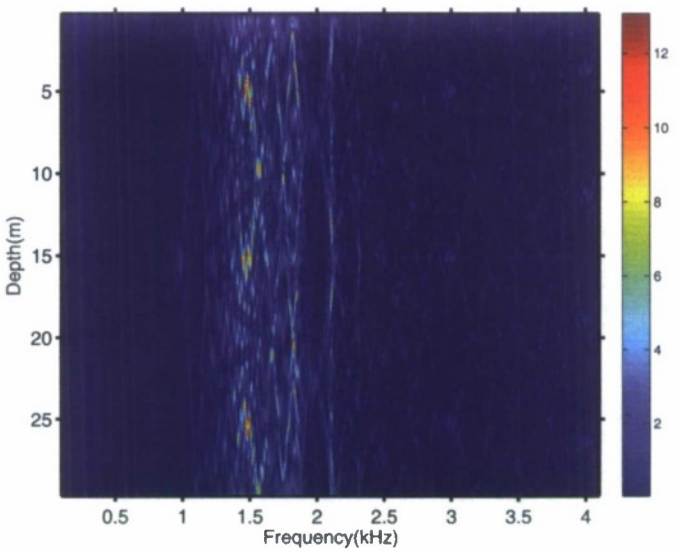

Figure 13: *The scattered field amplitude (scaled by $6 * 10^4$) as function of frequency and sphere depth for a range of 600 m.*

for the seabed, measured off the horizontal. Then the cycle distance corresponding to that angle is

$$r_c = 2h/tan(\theta_c) \tag{50}$$

For our example, the cycle distance is about 112 m. For the multipaths , which correspond to steeper angle than this, they will quickly die out due to the power of the reflection coefficient, which is less than one in this case. Thus, for a range of 600 m, approximately 6 terms should suffice. To be on the safe side, we will consider 8. In the previous example, at 100 m range, we simply used the frequency spacing of 10 Hz at which the free space scattering coefficients were computed. At longer ranges, this frequency spacing is not sufficiently fine, due to the larger travel time differences of the paths. In Figs.13-14, we show the resulting spectral and time pulse computations for a range of 600 m. The time series have been scaled by a factor of 6 which makes their amplitudes approximately equal to those for the 100 m case. In this approach we simply took a brute force approach of computing the scattering coefficients a_k at a spacing of 1 Hz. However, in order to speed the computations for subsequent computations, we have rearranged the original code (which was vectorized with respect to the sphere position) so that for a fixed sphere depth and a particular multipath arrival/scatter type, all the frequency computations are done in a vectorized form. Many of the terms are frequency independent and need be computed only once.

Finally, we consider a source with a bandwidth of 80 KHz. The spectrum of the direct return is that of Fig. 1 (weighted by the spectrum of the source). The range is 100 m

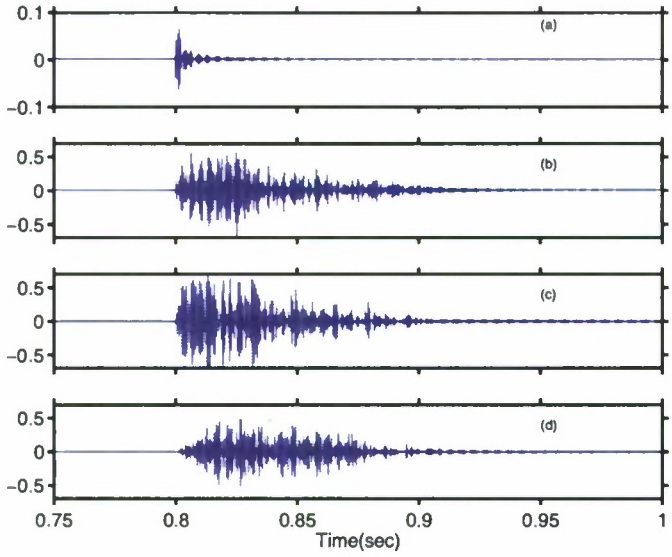

Figure 14: *Representative time series (scaled by a factor of 6) for (a) the free space echo (b) the sphere at 10 m depth (c) the sphere at 15 m depth and (d) the sphere at 29.7 m depth for a range of 600 m.*

but now the source/receiver is 2 m above the seabed. In Fig.15 we show the resulting spectra as a function of frequency and sphere depth for the first [100 4100] Hz, corresponding to the first example we considered, but with a different source/receiver depth. This is a "zoom " of this region contained within the much larger [100 80100] Hz interval shown in Fig. 17. As can be seen, the interference patterns seen in this case are quite different then the source/receiver being a midwater depth. Some selected time series are shown in Fig. 16. For the case of the sphere on the seabed, it is predicted that there will be virtually no direct arrival energy due to the constructive interference of the seabed reflected energy. The resulting backscattered spectra as a function of sphere depth and frequency are shown in Fig. 17 for the entire 80 kHz bandwith. The resulting time series, for a Gaussian pulse centred at 40.1 KHz and a bandwidth of 20 kHz, are shown in Fig. 18. For these higher frequencies and larger bandwith, the individual arrivals seem better resolved. However, there is still confusion because each multipath arrival consists of its own sequence of arrivals, due to the elastic/structural scattering of the sphere. In Fig. 19 a zoom of the time series near the specular reflection are shown for (a) just the direct paths and (b) for all paths, for the case of the sphere centre 0.3 mn above the seabed. It can be seen in (b) that the first echo appears to be different due to the coherent combination of the direct and the seabed reflected paths. This alteration of the specular echo was observed with real data and discussed in Ref. 5.

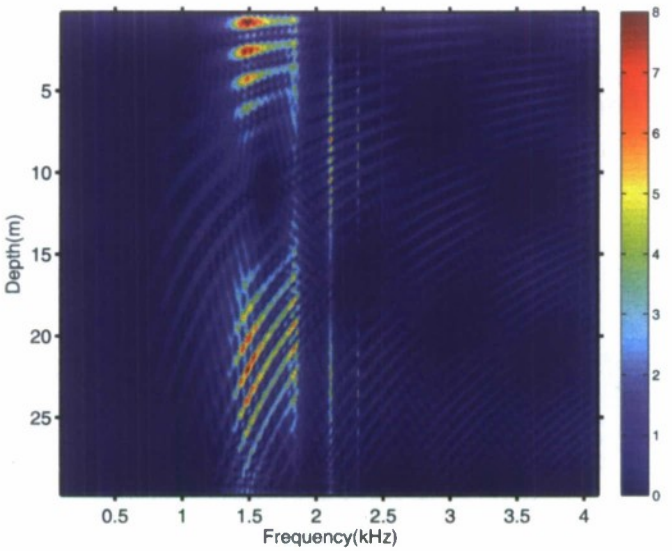

Figure 15: *The scattered field amplitude (scaled by 10^4) as function of frequency and sphere depth for a range of 100 m and source/receiver at 2 m above the seabed.*

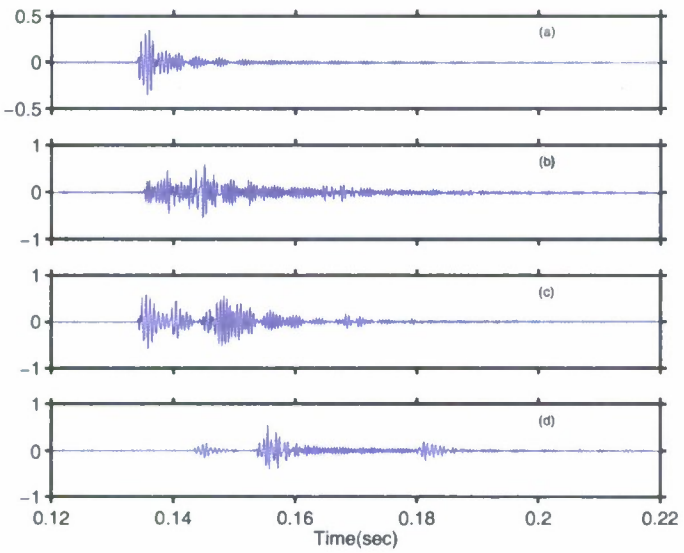

Figure 16: *Representative time series for (a) the free space echo (b) the sphere at 10 m depth (c) the sphere at 15 m depth and (d) the sphere at 29.7 m depth for a range of 100 m. The source function was a Gaussian pulse centred in [100 4100] Hz. The source/receiver are at 2 m above the seabed.*

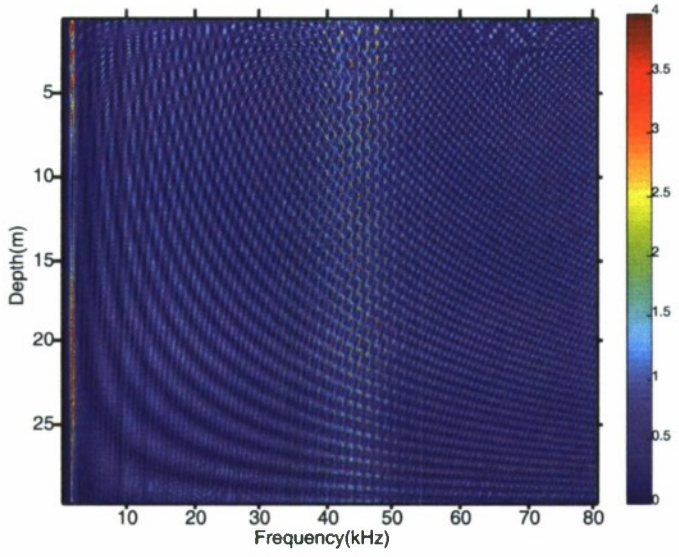

Figure 17: *The scattered field amplitude (scaled by 10^4) as function of frequency and sphere depth for a range of 100 m and source/receiver at 2 m above the seabed.*

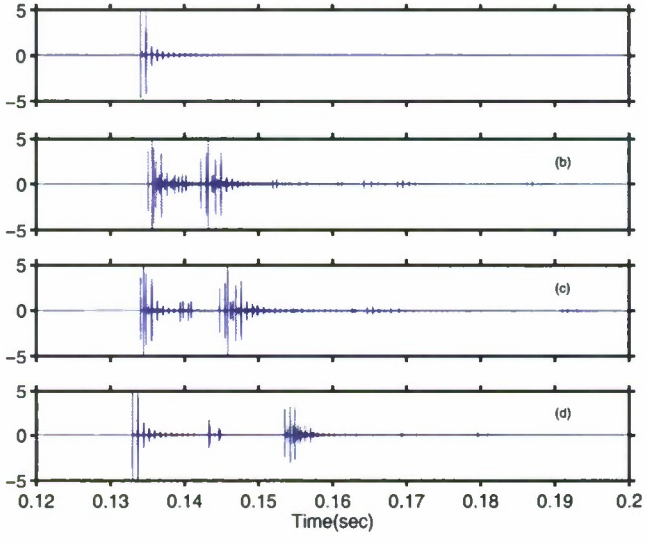

Figure 18: *Representative time series for (a) the free space echo (b) the sphere at 10 m depth (c) the sphere at 15 m depth and (d) the sphere at 29.7 m depth for a range of 100 m. The source function was a Gaussian pulse centred at 40100 Hz with a standard deviation of 20 kHz. The source/receiver are at 2 m above the seabed*

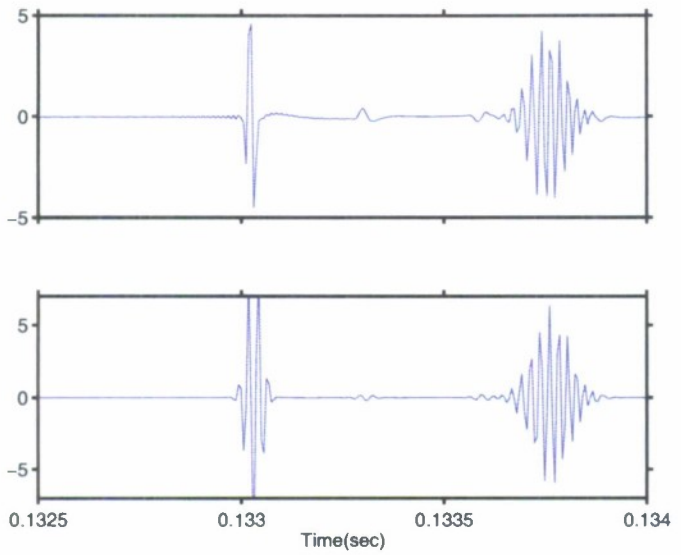

Figure 19: *. A zoom of the echo for (a) direct paths only (b) all paths for the region of the specular reflection. The source function was a Gaussian pulse centred at 40100 Hz with a standard deviation of 20 kHz. The source/receiver are at 2 m above the seabed*

4 SUMMARY

We have shown in this paper how the scattering by a spherical elastic shell can be accurately modelled within a simple Pekeris waveguide. It was found that the rescattering terms of the sphere with the surrounding boundaries could be significant for the sphere very close to a boundary (in our example, the upper surface). It was found that for frequencies greater than about 500 Hz, that a multipath/image solution could be used to model the propagation and scattering. The propagation effects within the waveguide and the sphere's depth in the waveguide alter the received echo significantly. In future work, we will use this model to examine the resulting possibilities for target classification.

References

[1] D.D. Sternlicht, A.W. Thompson, D.W. Lemonds, R.D. Dikeman, and M.T. Korporaal, "Image and signal classifcation for a buried object scanning sonar", *in Proceedings of IEEE/MTS Oceans 2002*, Vol.1, pp.485-490, (2002).

[2] F.B. Shin, D.H. Kil, and R.F. Wayland, "Active impulsive echo discrimination in shallow water by mapping target physics-based features to classifiers", IEEE

Journal of Oceanic Engineering, Vol.22, pp.66-80, 1997.

[3] P. Runkle, L. Carin, L. Couchman, J. Bucaro, and T. Yoder, "Multi-aspect identification of submerged elastic targets via wave-based matched pursuits and hidden Markov models", J. Acoust Soc., Vol. 106, pp. 605-616.

[4] J. Sildam and J. fawcett, "Baseline classification of acoustical signatures of mine-like objects", DRDC Atlantic TM 2005-058, July 2005.

[5] J.A. Fawcett, W.L.J. Fox, and A. Maguer, "Modeling of scattering by objects on the seabed", J. Acoust. Soc. Am., Vol. 104, pp.3296-3304 (1998).

[6] J.A. Fawcett, "Modelling of high-frequency scattering from elastic spheres", DREA TM 98-233, February, 1999.

[7] G.S. Sammelmann and R.H. Hackman, "Acoustic scattering in a homogenous waveguide", J. Acoust. Soc. Am., Vol.82, pp.324-336, 1987.

[8] R.H. Hackman and G.S. Sammelmann, "Multiple-scattering analysis for a target in an oceanic waveguide", J. Acoust. Soc. Am., Vol.84, pp. 1813-1825, 1988.

[9] N.C. Makris, "A spectral approach to 3-D object scattering in layered media applied to scattering from submerged spheres", J. Acoust. Soc. Am., Vol.104, pp.2105-2113, 1998.

[10] Y. Lai and N.C. Makris, "Spectral and modal formulations for the Doppler-shifted field scattered by an object moving in a stratified medium", J. Acoust. Soc. Am., Vol. 113, pp.223-244, 2003.

[11] K.V. Rao, N.M. Kee, P.W. Goalwin , and H. Schmidt, "Element level simulation of sonar echo from a moving target in an ocean waveguide", *in Proceedings of IEEE/MTS Oceans 94*, Vol.3, pp. 195-199, 1994.

[12] G.V. Frisk, *Ocean and seabed acoustics: A theory of wave propagation*, PTR Prentice Hall, 1994.

[13] F. Ingenito, "Scattering from an object in a stratified medium", J. Acoust. Soc. Am., Vol. 82, pp.2851-2859 (1987).

[14] W.G. Neubauer, *Acoustic reflection from surfaces and shapes*, Naval Research Laboratory, Washington, D.C., U.S.A., 1986.

[15] E.K. Westwood and C.T. Tindle, "Shallow water time-series simulation using ray theory", J. Acoust. Soc. Am., Vol.61, pp. 1752-1761, 1987.

Distribution List

Internal Distribution

1 Francine Desharnais,GL/MHD

1 John Fawcett

1 Juri Sildam

5 Library

Total internal copies: 8

External Distribution

1 NDHQ/DRDKIM

Total external copies: 1

Total copies: 9

This page intentionally left blank.

DOCUMENT CONTROL DATA

(Security classification of title, body of abstract and indexing annotation must be entered when document is classified)

1. ORIGINATOR (the name end eddress of the orgenization preparing the document. Organizations for whom the document was prepared, e.g. Centre sponsoring e contractor's report, or tasking egency, ere entered in section 8.)

   Defence R&D Canada – Atlantic
   P.O. Box 1012, Dartmouth, Nova Scotia, Canada B2Y 3Z7

2. SECURITY CLASSIFICATION (overall security clessification of the document including speciel warning terms if epplicable).

   UNCLASSIFIED

3. TITLE (the complete document title es indicated on the title page. Its clessification should be indicated by the eppropriete abbrevietion (S,C,R or U) in parentheses efter the title).

   Modelling broadband scattering from shelled spheres in a waveguide

4. AUTHORS (lest neme, first neme, middle initiel)

   Fawcett, John A.

5. DATE OF PUBLICATION (month end yeer of publication of document)	6a. NO. OF PAGES (totel conteining informetion. Include Annexes, Appendices, etc).	6b. NO. OF REFS (totel cited in document)
October 2007	38	15

7. DESCRIPTIVE NOTES (the category of the document, e.g. technical report, technical note or memorandum. If eppropriete, enter the type of report, e.g. interim, progress, summery, annual or final. Give the inclusive dates when e specific reporting period is covered).

   Technical Memorandum

8. SPONSORING ACTIVITY (the name of the department project office or laboratory sponsoring the reseerch end development. Include eddress).

   Defence R&D Canada – Atlantic
   P.O. Box 1012, Dartmouth, Nova Scotia, Canada B2Y 3Z7

9a. PROJECT NO. (the applicable reseerch end development project number under which the document was written. Specify whether project).	9b. GRANT OR CONTRACT NO. (if appropriete, the applicable number under which the document wes written).
11CF	

10a. ORIGINATOR'S DOCUMENT NUMBER (the officiel document number by which the document is identified by the origineting activity. This number must be unique.)	10b. OTHER DOCUMENT NOs. (Any other numbers which may be essigned this document either by the originator or by the sponsor.)
DRDC Atlantic TM 2007-270	

11. DOCUMENT AVAILABILITY (eny limitetions on further dissemination of the document, other than those imposed by security clessification)

   (X) Unlimited distribution
   ( ) Defence departments and defence contractors; further distribution only as approved
   ( ) Defence departments and Canadian defence contractors; further distribution only as approved
   ( ) Government departments and agencies; further distribution only as approved
   ( ) Defence departments; further distribution only as approved
   ( ) Other (please specify):

12. DOCUMENT ANNOUNCEMENT (eny limitetion to the bibliographic announcement of this document. This will normally correspond to the Document Availebility (11). However, where further distribution beyond the eudience specified in (11) is possible, e wider announcement eudience may be selected).

13. ABSTRACT (e brief end factuel summery of the document. It mey elso eppeer elsewhere in the body of the document itself. It is highly desirable that the abstract of clessified documents be unclassified. Eech paragraph of the ebstract shell begin with en indication of the security clessification of the informetion in the paragraph (unless the document itself is unclessified) represented es (S), (C), (R), or (U). It is not necessary to include hera abstracts in both official languages unless tha text is bilingual).

The broadband scattering characteristics of a target may be used to distinguish echos from a target of interest from those of clutter. This type of classification is of interest in many sonar applications: ASW, torpedo, surface mines, and diver detection. In a shallow water situation the original sonar pulse and the echo from the target will consist of a sequence of pulses corresponding to the various combinations of incident and backscattered multipath arrivals. For a very shallow target or one close to the seabed, it may be difficult to isolate some of these multipath arrivals. It is expected that these waveguide effects could have a significant effect upon some classifiers. In this paper, we discuss the modelling of scattering of sound from an elastic sphere (shelled, solid, water-filled, etc) which is in a waveguide with an upper surface and a lower seabed. An exact propagation solution is implemented and used to benchmark a ray-expansion solution. The scattered signals for a variety of different sonar pulses and different positions of a spherical target in the waveguide are shown.

14. KEYWORDS, DESCRIPTORS or IDENTIFIERS (technically meeningful terms or short phrases that cheracteriza e document and could be helpful in cataloguing tha document. They should be selected so that no security classification is required. Identifiers, such as equipment model designation, trade nama, military project coda nama, geographic location may also be included. If possible keywords should be selected from a published thesaurus. e.g. Thesaurus of Engineering and Sciantific Tarms (TEST) and that thesaurus-identified. If it not possibla to select indexing terms which are Unclassifiad, tha classification of each should ba indicated es with the title).

sphere, waveguide, scattering

This page intentionally left blank.

Defence R&D Canada

Canada's leader in defence
and National Security
Science and Technology

R & D pour la défense Canada

Chef de file au Canada en matière
de science et de technologie pour
la défense et la sécurité nationale

www.drdc-rddc.gc.ca